Research Square

Preprints are preliminary reports that have not undergone peer review.
They should not be considered conclusive, used to inform clinical practice,
or referenced by the media as validated information.

Synthesis of a Hydroxy-Functionalized Poly(m-xylylene) via Visible-Light-Driven Reductive Coupling of Isophthalaldehyde using Perylene as a Photoredox Catalyst

Shusuke Okamoto
University of Shizuoka
Seito Nose
Kindai University
Atsushi Sudo
asudo@emat.kindai.ac.jp

Kindai University

Research Article

Keywords:

Posted Date: June 19th, 2026

DOI: https://doi.org/10.21203/rs.3.rs-9846180/v1

License: This work is licensed under a Creative Commons Attribution 4.0 International License.
Read Full License

Additional Declarations: No competing interests reported.

Synthesis of a Hydroxy-Functionalized Poly(*m*-xylylene) via Visible-Light-Driven Reductive Coupling of Isophthalaldehyde using Perylene as a Photoredox Catalyst

Shusuke Okamoto[1], Seito Nose[2], and Atsushi Sudo[2]*

[1] School of Food and Nutritional Science, University of Shizuoka, Yada 52-1, Suruga-ku, Shizuoka, Shizuoka, 422-8526, Japan.
[2] Graduate School of Science and Engineering, Kindai University, Kowakae 3-4-1, Higashi Osaka, Osaka 577-8502, Japan.

Correspondence: Atsushi Sudo (E-mail: asudo@emat.kindai.ac.jp)

Abstract

A visible-light-driven synthesis of hydroxy-functionalized poly(*m*-xylylene) was developed via the reductive coupling of isophthalaldehyde, an aromatic dialdehyde. In this system, perylene served effectively as a photoredox catalyst under blue-light irradiation. It was found that selecting Hantzsch ester capable of activating the aldehyde substrate through hydrogen bonding is crucial for achieving sufficient polymer growth. MALDI-TOF MS analysis of the resulting polymers enabled detailed structural characterization of the polymer chain ends, revealing that their structures vary depending on the type of electron donor used. The obtained hydroxy-functionalized poly(*m*-xylylene)s exhibited glass transition temperatures above 100 °C, suggesting that hydrogen bonding between hydroxyl groups restricts polymer chain mobility.

Introduction

The reductive coupling of carbonyl compounds is a straightforward approach to the synthesis of 1,2-diols, which serve as precursors to pharmaceuticals, natural products, and agrochemicals, as well as important building blocks in organic synthesis. [1] In conventional reductive coupling methods, ketyl radical anions generated by single-electron reduction with stoichiometric amounts of reducing agents undergo radical-radical coupling, followed by hydrogen-atom abstraction, to afford the corresponding 1,2-diol. [2-4]

Recently, photoredox catalysts (PRCs) have emerged as an important tool for the environmentally benign synthesis of valuable molecules by promoting both oxidation and reduction processes under light irradiation. [5,6] Metal-based complexes such as iridium [7], copper [8], and samarium [9] complexes have been widely employed for the light-driven reductive coupling of carbonyl compounds. In parallel, the demand for greener catalysts has spurred the use of π-conjugated organic dyes as metal-free PRCs, which now constitute a major class of catalysts for light-mediated transformations [10-20]. In both the oxidative and reductive cycles of these PRC systems, the generation of ketyl radical anions via single-electron transfer (SET) is a key step in the reductive coupling process. We have previously reported that perylene and its derivatives function as PRCs for the visible-light-driven reductive coupling of aromatic carbonyl compounds to afford the corresponding 1,2-diols [21-23] (Figure 1A). The efficient progress of this coupling reaction motivated us to extend this system to reductive coupling polymerization under visible-light irradiation.

Hydroxy-functionalized poly(xylylene)s, which consist of repeating 1,2-diol units, possess hydroxyl groups on their side chains and are promising for the development of functional polymer materials. Hydroxy-functionalized poly(*p*-xylylene)s have been

synthesized by the reductive coupling polymerization of aromatic dialdehydes using divalent samarium compounds [24]. To the best of our knowledge, no PRC-based reductive coupling polymerization system has yet been reported.

In this paper, we report the synthesis of hydroxy-functionalized poly(*m*-xylylene)s via the visible-light-driven reductive coupling polymerization of isophthalaldehyde, an aromatic dialdehyde, using a perylene-based PRC system (Figure 1B).. The resulting polymers, hydroxy-functionalized poly(*m*-xylylene)s bearing 1,2-diol structures in their repeating units, were analyzed by MALDI-TOF MS, which enabled detailed structural characterization of the chain ends. Among them, the polymer with the highest number-average molecular weight was subjected to thermogravimetric analysis (TGA) and differential scanning calorimetry (DSC).

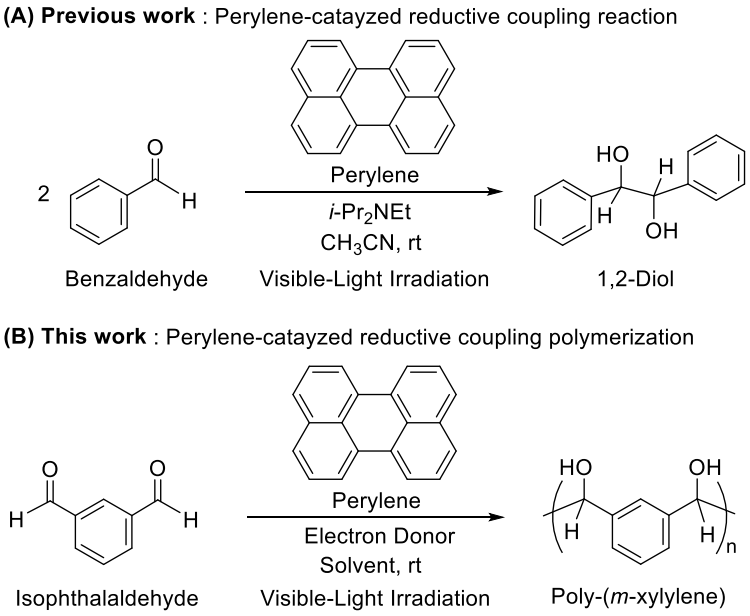


Figure 1. (A) Visible-light-driven reductive coupling reaction of benzaldehyde using perylene. (B) Visible-light-driven reductive coupling polymerization of isophthalaldehyde using perylene.

Experimental

Materials

Anisole (99.0%), isophthalaldehyde (92%), perylene (95.0%), and calcium hydride (96.0%), chloroform (99.0%), sodium iodide (99.5%), toluene (99.5%), and 1,8,9-trihydroxyanthracene were purchased from Wako Pure Chemical Industries, Ltd. and used as received. Chloroform-d_1 (99.8%, containing 0.03% TMS) and dimethyl sulfoxide-d_6 (DMSO-d_6) (99.9%, containing 0.03% TMS) were purchased from Kanto Chemical Co., Inc. and used as received. 1,4-Dihydro-2,6-dimethyl-3,5-pyridinedicarboxylic acid diethyl ester (Hantzsch ester; HE) (98.0%), and 1,4-dihydro-2,6-dimethyl-3,5-pyridinedicarboxylic acid di-*tert*-butyl ester (HE-TB) (98.0%) were purchased from Tokyo Chemical Industry Co., Ltd. and used as received. *N*,*N*-dimethylformamide (DMF) (>99.5%, anhydrous) was distilled over calcium hydride prior to use. *N*,*N*-diisopropylethylamine (DIPEA) (>97.0%) was purchased from Wako Pure Chemical Industries, Ltd. and distilled over sodium hydroxide prior to use. Benzaldehyde (98.0%) was purchased from Wako Pure Chemical Industries, Ltd. and distilled under reduced pressure prior to use.

Instruments

NMR spectra (600 MHz for ^{1}H) were recorded on a Bruker AVANCE 600 spectrometer. Chemical shifts (δ) and coupling constants (J) are reported in ppm and Hz, respectively. A blue tape light (30 LEDs, 1 m; Daiso Industries Co., Ltd.) was used as the light source. Number-average molecular weights (M_n) and weight-average molecular weights (M_w) were estimated by size exclusion chromatography (SEC) using a TSKgel Super HM-H column (6.0 mm × 15 cm; Tosoh Co.) equipped with a Tosoh HLC-8320 GPC system. DMF containing 1 wt% lithium bromide was used as the eluent at a flow rate of 0.6 mL/min, and calibration was performed with polystyrene standards. Thermogravimetric analysis (TGA) was performed on a Shimadzu DTG-60 thermal analyzer under a nitrogen

atmosphere. The sample was heated from 50 °C to 500 °C at a rate of 10 °C/min. Differential scanning calorimetry (DSC) was performed on a Shimadzu DSC-60 Plus under a nitrogen atmosphere. The sample was first heated from –50 °C to 250 °C, depending on the thermal stability of the polymer, then cooled to 0 °C at 30 °C/min. DSC data was collected by reheating the sample from 0 °C at a rate of 10 °C/min. The glass-transition temperature (T_g) was determined as the extrapolated onset temperature from the obtained DSC profile. MALDI-TOF-MS spectra were recorded on a Shimadzu model AXIMA Confidence. The details of the density functional theory (DFT) calculations were described in the Supporting Information.

Visible-light-driven reductive coupling reaction of benzaldehyde 1

According to our previous report [23], benzaldehyde **1** (102.0 mg; 0.9612 mmol), perylene (7.2 mg; 0.030 mmol), HE (256.2 mg; 1.011 mmol), and DMF (12.5 mL) were placed in a 50 mL round-bottom flask, degassed by sonication under reduced pressure, and subsequently purged with argon. The solution was then stirred at room temperature under blue LED irradiation for 18 h. The conversion of **1** and the yield of 1,2-diol **2** were determined by crude ^{1}H NMR analysis using anisole (103.9 mg; 0.9612 mmol) as an internal standard. ^{1}H NMR (600 MHz, $CDCl_3$, r.t., ppm) δ 7.11–7.34 (m, 20H, *meso* and *dl*), 4.83 (s, 2H, *meso*) 4.71 (s, 2H, *dl*) 2.86 (s, 2H, *meso*) 2.22 (s, 2H, *dl*). The ^{1}H NMR spectrum was consistent with the previously reported data. [7-23]

Visible-light-driven reductive coupling polymerization of isophthalaldehyde 3

Entry 1 of Table 1

General procedure; visible-light-driven reductive coupling polymerization of isophthalaldehyde **3** (134.0 mg; 0.9990 mmol) was carried out using perylene (14.6 mg; 0.0579 mmol) in the presence of DIPEA (0.35 mL; 2.0 mmol) in DMF (25 mL) at room temperature under an argon atmosphere and blue LED irradiation for 48 h. The reaction

mixture was concentrated under reduced pressure to afford a brown solid. The obtained solid was dissolved in DMF (2 mL) and precipitated by dropwise addition into toluene (100 mL), followed by stirring for 30 min. The resulting solid was isolated by suction filtration to give hydroxy-functionalized poly(*m*-xylylene) **4** as a brown solid (21.8 mg; 16% of the theoretical yield): ^{1}H NMR (600 MHz, DMSO-d_6, r.t., ppm) δ 6.48-7.57 (br, 4H), 4.84-5.47 (br, 2H), 4.19-4.66 (br, 2H), M_n (g/mol) = 1100, M_w/M_n = 1.6.

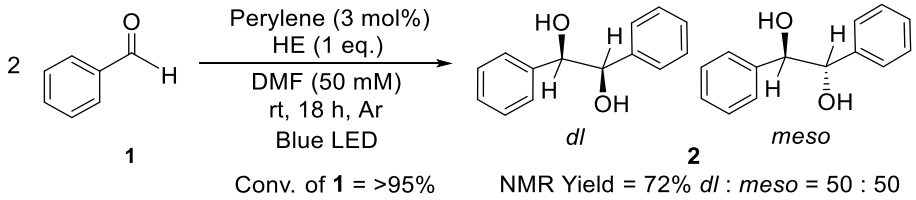
Entry 2 of Table 1

According to the general procedure, the visible-light-driven reductive coupling polymerization of **3** (134.6 mg; 1.004 mmol) was carried out using perylene (14.9 mg; 0.0591 mmol) in the presence of HE (507.8 mg; 2.005 mmol) in DMF (25 mL). The reaction mixture was concentrated under reduced pressure, and the obtained solid was dissolved in DMF (3.5 mL) and precipitated into chloroform (200 mL) with stirring for 30 min. The resulting solid was isolated by suction filtration to afford **4** as a yellow solid (80.7 mg; 60% of the theoretical yield): ^{1}H NMR (600 MHz, DMSO-d_6, r.t., ppm) δ 6.48-7.57 (br, 4H), 4.84-5.47 (br, 2H), 4.19-4.66 (br, 2H), IR (KBr, cm^{-1}) 3383, 2884, 1658, 1029, 705, M_n (g/mol) = 3700, M_w/M_n = 1.5.

Entry 3 of Table 1

According to the general procedure, the visible-light-driven reductive coupling polymerization of **3** (134.9 mg; 1.005 mmol) was carried out using perylene (15.2 mg; 0.0602 mmol) in the presence of HE-TB (621.2 mg; 2.008 mmol) in DMF (25 mL). The reaction mixture was concentrated under reduced pressure, and the obtained solid was dissolved in DMF (3.5 mL) and precipitated into toluene (120 mL) with stirring for 30 min. The resulting solid was isolated by suction filtration to afford **4** as a yellow solid (97.7 mg; 72% of the theoretical yield): ^{1}H NMR (600 MHz, DMSO-d_6, r.t., ppm) δ 6.48-7.57 (br, 4H), 4.84-5.47 (br, 2H), 4.19-4.66 (br, 2H), M_n (g/mol) = 3300, M_w/M_n = 1.6.

Results and Discussion



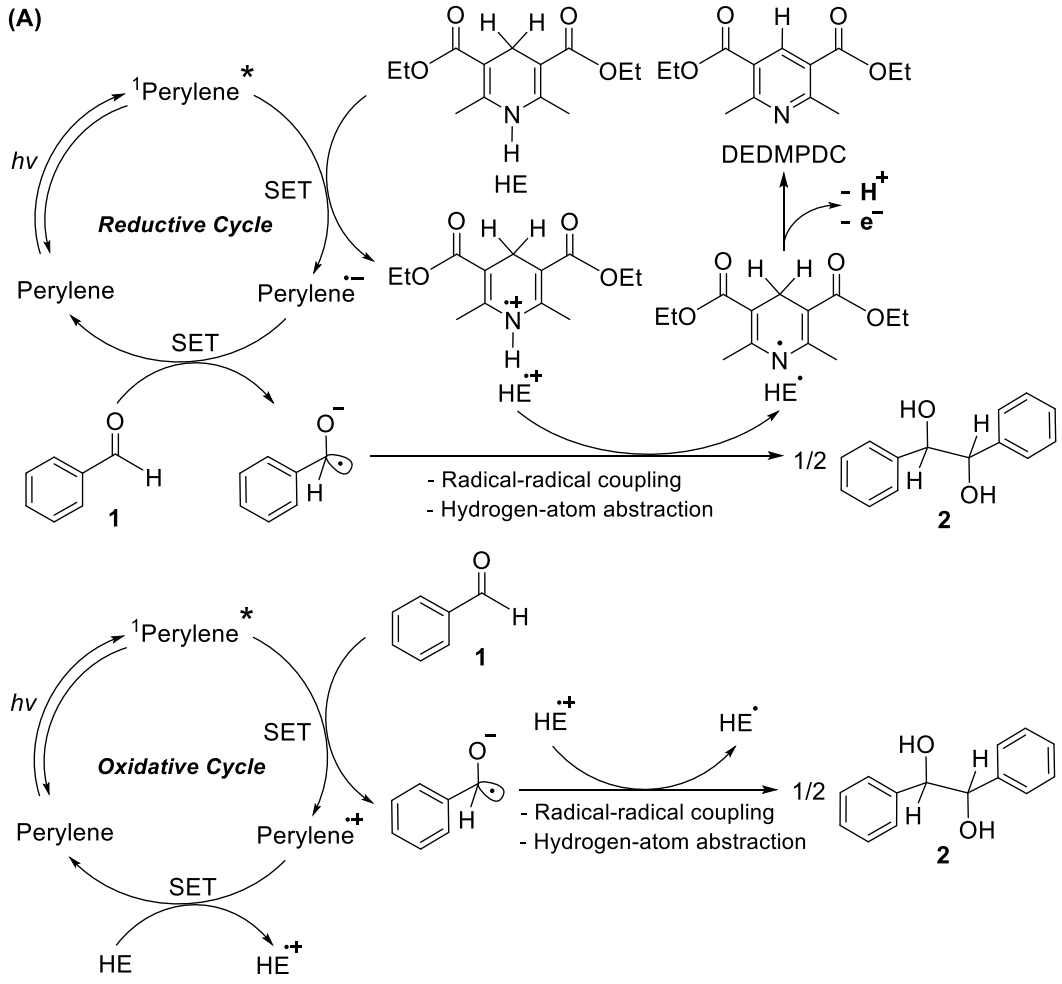
Scheme 1. Visible-light-driven reductive coupling of benzaldehyde **1**.

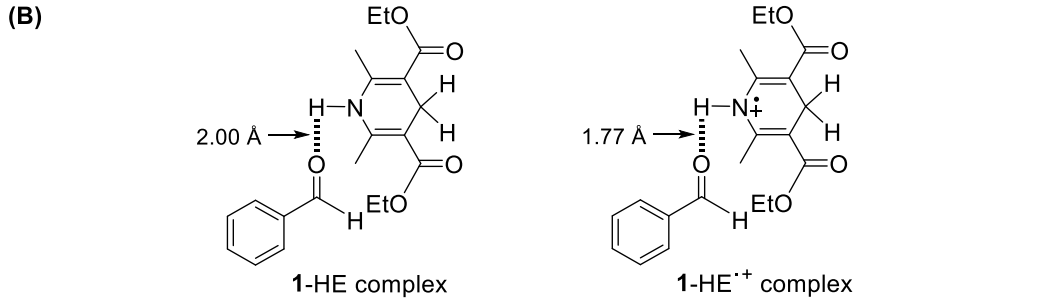
In previous studies on visible-light-driven reductive coupling of aldehydes using perylene as a photoredox catalyst (PRC), acetonitrile has been employed as the solvent. In the present study, however, DMF was selected as the solvent because it is expected to reliably dissolve the hydroxyl-functionalized polymer to be synthesized. Accordingly, the reaction efficiency of the reductive coupling of benzaldehyde in DMF was investigated. In addition, Hantzsch ester (HE), a 1,4-dihydropyridine derivative, was employed as the electron donor for the reductive coupling due to its established use in various photoredox systems and the potential for recovery and reuse of the resulting pyridine derivative [25].

As shown in Scheme 1, he visible-light-driven reductive coupling of benzaldehyde **1** was carried out using 3 mol% perylene in the presence of 1 equivalent amount of HE as an electron donor in DMF under an argon atmosphere with blue LED irradiation, affording the corresponding 1,2-diol **2**. The crude ^{1}H NMR analysis showed quantitative consumption of **1** and formation of **2** (Figure S1). The NMR yield of **2** was 72%, and its *dl*-to-*meso* ratio was 50:50. These results suggested that HE functions as an electron donor in the perylene-based PRC system, as does DIPEA [23].

Since perylene undergoes both reversible oxidation and reduction potentials ($E_{1/2}$(perylene$^{\bullet+}$/perylene) = 0.85 V vs SCE in CH_3CN and $E_{1/2}$(perylene/perylene$^{\bullet-}$) = -1.67 V vs SCE in DMF/CH_3CN) [26], two plausible mechanisms can be proposed for the perylene-catalyzed reductive coupling of **1** (Figure 2A). First, a mechanism involving a

reductive catalytic cycle is considered. Upon visible-light irradiation, perylene is converted to its excited state (perylene*). The singlet excited-state reduction potential of perylene (E^*_{red} = 0.72 V vs. Cp_2Fe in CH_3CN, corresponding to ca. 1.12 V vs. SCE) [27] is more positive than the oxidation potential of HE ($E_{pa/2}$ = 0.72 V vs. SCE in CH_3CN) [28], suggesting that single-electron transfer (SET) from HE to ^{1}perylene* occurs to generate the radical anion of perylene (perylene$^{\bullet-}$) and the radical cation of HE (HE$^{\bullet+}$) (Figure 2A). Subsequently, SET from perylene$^{\bullet-}$ to **1** generates the radical anion of **1**, although the ground-state reduction potential of perylene ($E_{1/2}$(perylene/perylene$^{\bullet-}$) is less negative than that of **1** ($E_{pc/2}$ = -1.93 V vs SCE) [29]. This can be attributed to activation of the carbonyl carbon in **1** through hydrogen-bonding interactions with HE and/or HE$^{\cdot+}$. A similar role of HE and/or HE$^{\bullet+}$ has been proposed in other PRC systems. [13-15,17] The radical anion of **1** then undergoes bimolecular radical-radical coupling, followed by hydrogen-atom abstraction from HE and/or HE$^{\bullet+}$, to afford the desired 1,2-diol **2** together with an HE-derived radical (HE$^{\bullet}$) as a byproduct. Furthermore, HE$^{\bullet}$ would act as both an electron donor and a proton source and be converted into diethyl 2,6-dimethylpyridine-3,5-dicarboxylate (DEDMPDC) [14,25]. Next, the possibility of an oxidative catalytic cycle is considered. The singlet excited-state oxidation potential (E^*_{ox} = -2.23 V vs. Cp_2Fe in CH_3CN, corresponding to ca. -1.78 V vs. SCE) [27] and the ground-state oxidation potential of perylene also support the possibility that the reductive coupling proceeds via an oxidative catalytic cycle (Figure 2A).

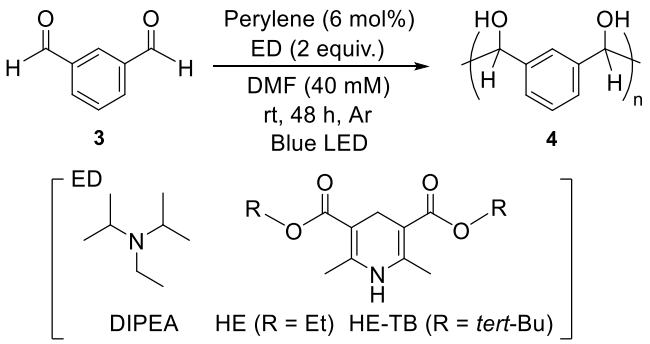




Substrate	LUMO (eV)	Electronic State of Carbonyl Carbon in **1**	Complexation Energy (kcal/mol)
1	-0.045	0.414	
1-HE complex	-0.231	0.424	-4.64
1-HE$^{\bullet+}$ complex	-0.459	0.434	-5.71

Figure 2. (A) Postulated mechanisms for visible-light-driven radical coupling reaction of **1**. (B) DFT-calculated LUMO energies and NPA charges in DMF of **1**, **1**-HE complex and **1**-HE$^{\bullet+}$ complex.

To clarify the effects of HE and $HE^{\bullet+}$ on the activation of **1**, density functional theory (DFT) calculations were performed on the **1**-HE and **1**-$HE^{\bullet+}$ complexes (Figures 2B and Figures S6-S9). Figure 2B shows that, in both complexes, the two components are positioned at distances conducive to hydrogen-bond formation. Compared with free **1**, **1** in both complexes exhibited lower LUMO energies. In contrast, the electronic states of the carbonyl carbon in free **1** and in the **1** moiety each of the two complexes were essentially unchanged, indicating that complexation does not substantially alter the local electrophilicity of the carbonyl carbon. These findings suggest that the interaction with HE or $HE^{\bullet+}$ promotes reduction mainly through stabilization of the LUMO rather than through direct polarization of the carbonyl carbon. The complexation energies of the **1**–HE and **1**–$HE^{\bullet+}$ complexes were calculated in the gas phase to be −7.34 and −20.08 kcal mol^{-1}, respectively, indicating that formation of both complexes is energetically favorable (Table S1). Even in DMF, the reaction solvent used in this study, the corresponding complexation energies remained negative at −4.64 and −5.71 kcal mol^{-1} (Figure 2B, Table S1), respectively, suggesting that both complexes can also form under the experimental conditions. The larger stabilization of the **1**–$HE^{\bullet+}$ complex indicates that oxidation of HE strengthens its interaction with **1**.



Scheme 2. Visible-light-driven reductive polymerization of isophthalaldehyde **3**.

Based on the reaction conditions for the visible-light-driven reductive coupling of **1**

(Scheme 1), visible-light-driven reductive coupling polymerization of isophthalaldehyde **3**, an aromatic dialdehyde monomer, was carried out in DMF using perylene and several electron donors under blue LED irradiation to afford the target hydroxy-functionalized poly(*m*-xylylene)s **4** (Scheme 2). The results are summarized in Table 1. The structures and molecular weights of **4** were characterized by NMR, IR, and SEC analyses (Figure 3 and Figures S2 and S3). The ^{1}H NMR spectra of the resulting polymers (Figure 3) exhibited signals attributable to aromatic and methine protons, consistent with the formation of **4**. Only **4** obtained using DIPEA showed signals corresponding to terminal formyl groups, indicating that 10% of the formyl groups remained unreacted. The isolated yield and molecular weight of **4** obtained using DIPEA were significantly lower than those obtained using HE and HE-TB (entries 1 vs entries 2 and 3). In contrast, the yields and molecular weights obtained using HE and HE-TB were comparable (entries 2 and 3). These results suggest that the polymerization efficiency depends on the electron donor used. These differences can be attributed to side reactions during the reductive coupling polymerization. Specifically, plausible side reactions include (1) radical-radical cross-coupling of the radical anion of **3** with a DMF-derived radical, an electron donor-derived radical, and/or its radical cation, and (2) hydrogen-atom abstraction from the electron donor and/or its radical cation by the radical anion of **3**. These reaction mechanisms will be discussed in detail later. In addition, the *dl* to *meso* ratios of **4** could not be determined clearly because the signals corresponding to the two types of methine protons, assigned as signals (***a***) in Figure 3, overlapped. The *dl* to *meso* ratios estimated from the integral ratios of the hydroxy protons assigned as signals (***b***) in Figure 3 were comparable to that of **2**. Thus, no significant diastereoselectivity appears to be operative during the polymerization under the present conditions.

The thermal properties of **4** obtained using HE were evaluated by TGA and DSC (Figures S4 and S5). The temperature at 10% weight loss (T_{d10}) and the glass-transition temperature (T_g) were 253 ºC and 106 ºC, respectively. The T_g value of **4** was much higher than the previously reported value for **4** with a number-average molecular weight of 1700, as estimated by ^{1}H NMR analysis (T_g = 43 ºC) [24]. This difference suggests that the increased molecular weight of **4** markedly restricts molecular mobility, thereby resulting in a higher T_g.

Table 1. Results of visible-light-driven reductive coupling polymerization of **3**.

Entry	Electron Donor	Residual ratio of formyl groups (%)[a]	Yield of **4** (%)[b]	M_n (g/mol)[d]	M_w/M_n[d]
1	DIPEA	10	16	1100	1.6
2	HE	0	60[c]	3700	1.5
3	HE-TB	0	72	3300	1.6

[a] Determined by ^{1}H NMR analysis. [b] Insoluble-parts in toluene. [c] Insoluble-parts in chloroform. [d] Estimated by SEC analysis (10 mM LiBr in DMF, polystyrene standards).

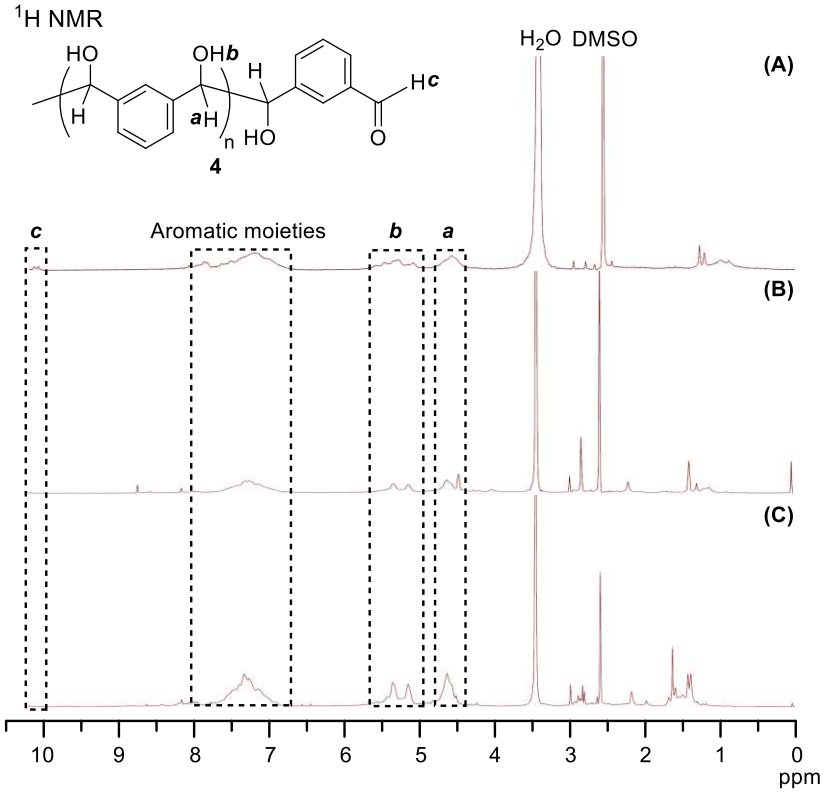


Figure 3. ^{1}H NMR spectra (600 MHz, DMSO-d_6) of hydroxy-functionalized poly(*m*-xylylene)s **4** obtained using (A) DIPEA, (B) HE, and (C) HE-TB.

To investigate how electron donors influence the polymerization behavior, MALDI-TOF MS analysis of **4** was performed using sodium iodide as the ionization agent and 1,8,9-trihydroxyanthracene as the matrix. The resulting spectra are shown in Figure 4. In all cases, peaks separated by m/z 136, corresponding to the repeating unit derived from **3**, were observed, indicating that the polymerization proceeded regardless of the electron donor used. By contrast, the choice of electron donor affected the terminal structures of **4**. When DIPEA was used, **4** bearing unreacted formyl groups at both chain ends was detected as peaks attributable to **Series A**. In addition, peaks assignable to **Series B** were attributed to **4** bearing an alcohol group which is formed by reduction of a formyl group at one chain end and a DMF-derived group at the other. When HE or HE-TB were used, the **Series A** peaks were absent, and new **Series A'** peaks assignable to **4** bearing cyclic structures appeared, suggesting that these electron donors are more suitable for this

polymerization than DIPEA. In the case of HE, peaks assignable to **Series C** were attributed to **4** bearing an alcohol group at one chain end and an HE-derived group at the other. When HE-TB was used, both **Series A′** and **Series B** peaks were observed. A detailed discussion of the influence of electron donors on the structure of **4** is provided in the following section describing the polymerization mechanism.

A plausible mechanism for the visible-light-driven reductive coupling polymerization is proposed in Figure 5. The polymerization of **3** affords **4** bearing formyl groups at both chain ends, corresponding to **Series A**, together with a propagating radical. The propagating radical is assumed to undergo three possible reaction pathways. In the first pathway, intramolecular cyclization of the propagating radical affords **4** containing cyclic structures, corresponding to **Series A'**. In the second pathway, the propagating radical couples with DMF-derived radicals generated during the polymerization, followed by hydrogen-atom abstraction, to afford **4**, corresponding to **Series B**. In the third pathway, the propagating radical couples with ED-derived radicals generated during the polymerization, followed by hydrogen-atom abstraction, to afford **4**, corresponding to **Series C**. Peaks assignable to Series C were observed for **4** obtained using HE, whereas such peaks were absent for **4** obtained using HE-TB. These results suggest that steric hindrance around the ester moiety influences coupling with the propagating radical.

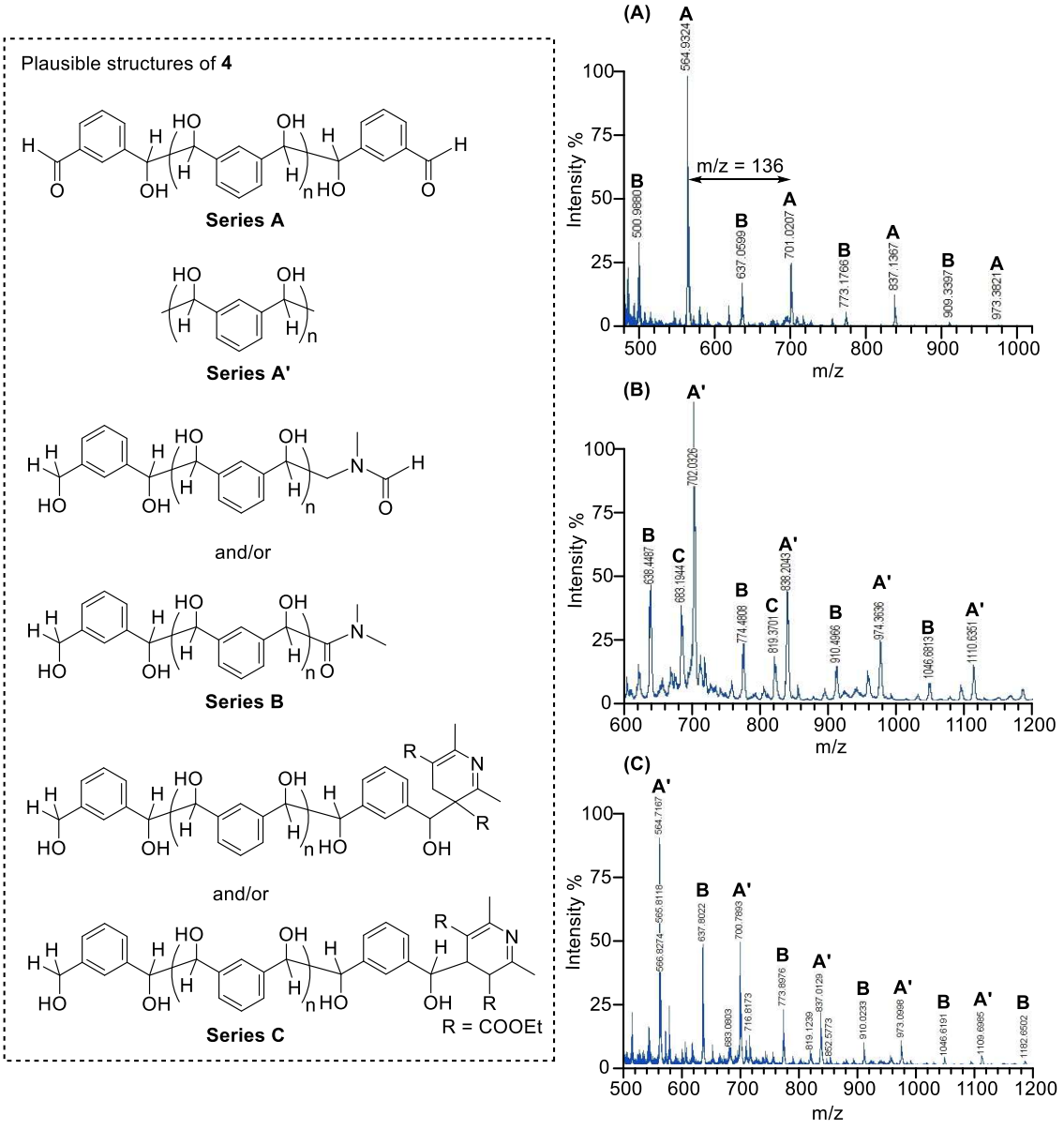


Figure 4. MALDI-TOF-MS spectra of hydroxy-functionalized poly(*m*-xylylene)s **4** using (A) DIPEA, (B) HE, and (C) HE-TB.

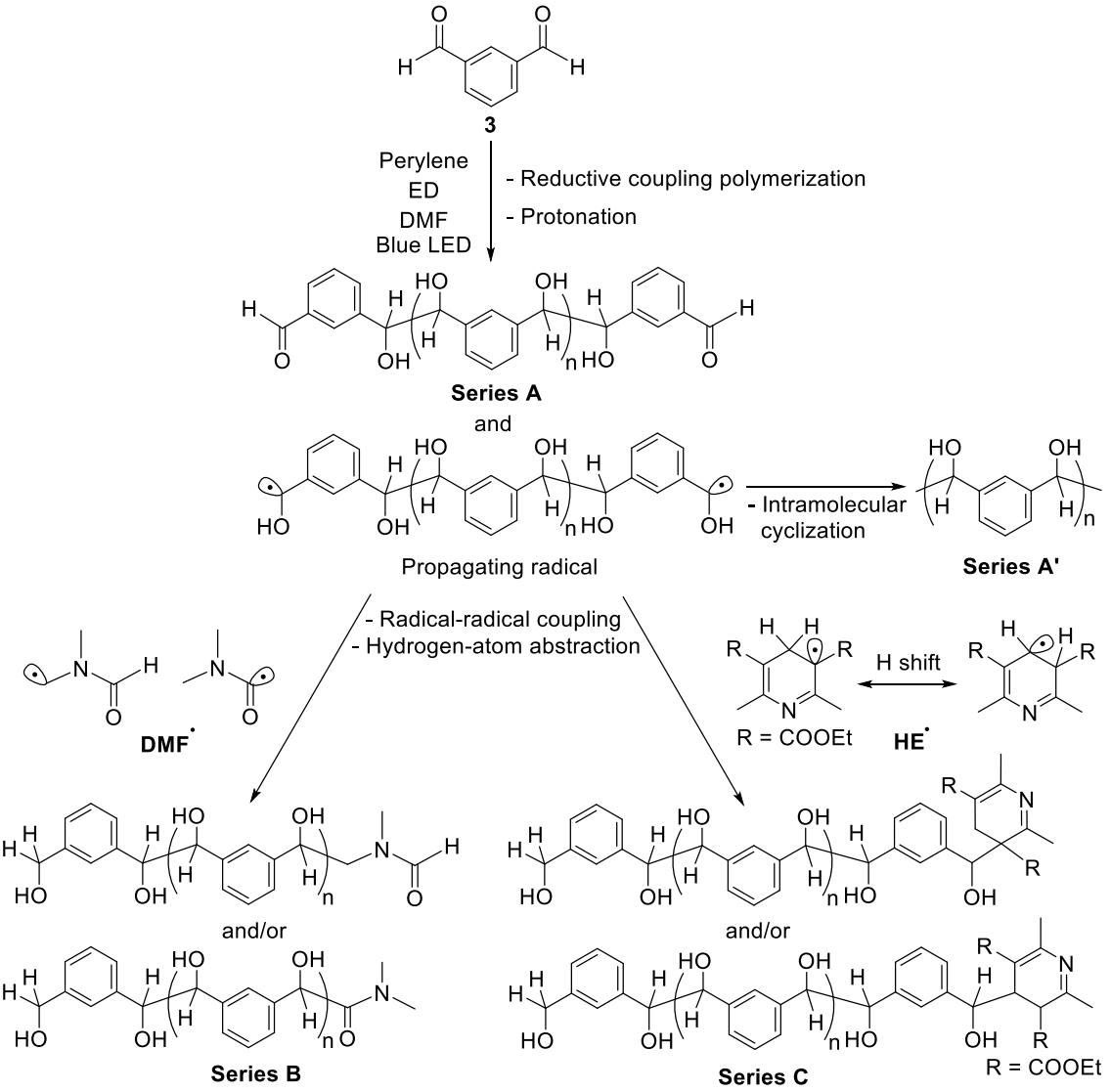
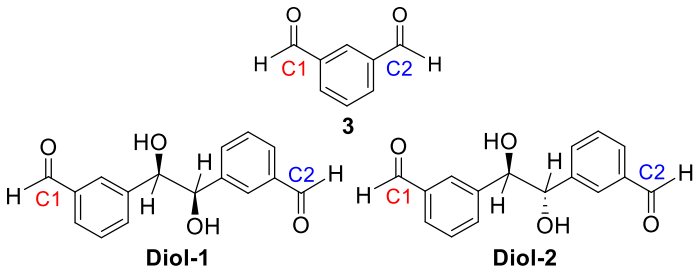


Figure 5. Possible mechanism for light-driven reductive coupling polymerization.

To clarify the factors limiting the molecular weight of **4** to the oligomeric range, DFT calculations were carried out for **3** and the model compounds **Diol-1** and **Diol-2**, which correspond to the repeating units of **4**, under the same computational conditions as those used for **1** (Figures S8 and S9). The results are summarized in Figure 6. The LUMO energies of **Diol-1** and **Diol-2** were comparable to each other and higher than that of **3**, indicating that **3** is more readily reduced than either **Diol-1** or **Diol-2**. The electronic states of the two carbonyl carbons in each of **3**, **Diol-1**, and **Diol-2** were also comparable. These

findings suggest that, although the local electronic properties of the carbonyl carbons remain essentially unchanged before and after reductive coupling, the reducibility of the molecules is altered. Because the LUMO energies and electronic states of the carbonyl carbons of **Diol-1** and **Diol-2** were comparable to those of **1**, reductive coupling polymerization was expected to remain feasible. However, the limited molecular-weight growth can be attributed to the restricted molecular mobility of the rigid oligomeric species, which decreases the probability of productive encounters between reactive sites during polymerization. Furthermore, substrate activation by the electron donor and/or its radical cation, as illustrated in Figure 2, is likely to influence the polymerization efficiency. Both HE and $HE^{\bullet+}$ can form hydrogen-bonding interactions with the formyl groups of **3** and the oligomeric species. In the case of DIPEA, however, such hydrogen-bonding interactions are expected to be mediated mainly by $DIPEA^{\bullet+}$. Neutral HE is not expected to suppress hydrogen-bond formation between HE or $HE^{\bullet+}$with the substrate, whereas the basicity of DIPEA may induce proton-transfer equilibrium between DIPEA and $DIPEA^{\bullet+}$, thereby reducing the availability of $DIPEA^{\bullet+}$ for hydrogen-bond formation with the substrate. This effect likely contributes to the lower polymerization efficiency of the DIPEA-based system compared with the systems using HE and HE-TB, resulting in lower molecular weights of the obtained polymers.



Substrate	LUMO (eV)	Electronic State of Carbonyl Carbon
3	-0.214	C1 : 0.416 C2 : 0.416
Diol-1	-0.044	C1 : 0.415 C2 : 0.415
Diol-2	-0.044	C1 : 0.414 C2 : 0.414

Figure 6. DFT-calculated LUMO energies and NPA charges in DMF of **3**, **Diol-1**, and **Diol-2**.

summary

In this study, we reported the synthesis of hydroxy-functionalized poly(*m*-xylylene)s via visible-light-driven reductive coupling polymerization of isophthalaldehyde catalyzed by perylene in the presence of electron donors under blue LED irradiation. Based on the optimized conditions for the visible-light-driven reductive coupling of benzaldehyde using perylene and HE, isophthalaldehyde underwent polymerization with high monomer conversion to afford the target hydroxy-functionalized poly(*m*-xylylene)s with oligomeric molecular weights. The polymer obtained using HE exhibited T_{d10} and T_g values of 253 °C and 106 °C, respectively. ^{1}H NMR and MALDI-TOF-MS analyses of the obtained polymers revealed that the electron donor used influenced the structures of the resulting polymers. In addition, DFT calculations supported the role of HE in the visible-light-driven reductive coupling system and identified a key factor limiting the reaction to oligomer formation. These findings demonstrate that the environmentally benign polymerization system developed in this study provides a new route to poly(*m*-xylylene) synthesis with broad potential applications in the design of functional materials.

Supplementary Information

The spectral copies (NMR, IR, SEC, TG, and DSC analyses) of the synthesized compounds and the computational results employing DFT calculations are described in supporting information.

Author contributions Seito Nose performed the syntheses and analyses. Shusuke Okamoto and Seito Nose wrote the main manuscript. Atsushi Sudo conceptualized this work, curated the data, and prepared the schemes, figures, and the supplementary information. All authors reviewed the manuscript.

Declarations

Competing interests The authors declare no competing interests.

Funding This work was supported by JSPS KAKENHI Grant Number 21K05174. The computation was performed using Research Center for Computational Science, Okazaki, Japan (Project: 25-IMS-C422).

Data availability No datasets were generated or analyzed during the current study.

References

1. Chatterjee A, Joshi N N (2006) Evolution of the stereoselective pinacol coupling reaction. Tetrahedron 62:12137-12158. https://doi:10.1016/j.tet.2006.09.002
2. Yoshimura A, Saeki T, Nomoto A, Ogawa A (2015) Pinacol couplings of a series of aldehydes and ketones with SmI_2/Sm/Me_3SiCl in DME. Tetrahedron 71:5347-5355. http://dx.doi.org/10.1016/j.tet.2015.06.007
3. Wang C, Pan Y, Wu A (2007) $InCl_3$/Al mediated pinacol coupling reactions of aldehydes and ketones in aqueous media. Tetrahedron 63:429-434. http:// doi:10.1016/j.tet.2006.10.061
4. Uchiyama M, Matsumoto Y, Nakamura S, Ohwada T, Kobayashi N, Yamashita N, Matsumiya A, Sakamoto T (2004) Development of a Catalytic Electron Transfer System Mediated by Transition Metal Ate Complexes: Applicability and Tunability of Electron-releasing Potential for Organic Transformations. Journal of the American Chemical Society 126:8755-8759. https://pubs.acs.org/doi/10.1021/ja039674a
5. Holmberg-Douglas N, Nicewicz D A (2022) Photoredox-Catalyzed C−H Functionalization Reactions. Chemical Reviews 126:1925-2016. https://doi.org/10.1021/acs.chemrev.1c00311
6. Prier C K, Rankic D A, MacMillan D W C (2013) Visible Light Photoredox Catalysis with Transition Metal Complexes: Applications in Organic Synthesis. Chemical Reviews 113:5322-5363. https:// dx.doi.org/10.1021/cr300503r

7. Nakajima M, Fava E, Loescher S, Jiang Z, Rueping M (2015) Photoredox-Catalyzed Reductive Coupling of Aldehydes, Ketones, and Imines with Visible Light. Angewandte Chemie International Edition 54:8828-8832. https://doi: 10.1002/anie.201501556
8. Caron A, Morin É, Collins S K (2019) Bifunctional Copper-Based Photocatalyst for Reductive Pinacol-Type Couplings. ACS Catalysis 9:9458-9464. https://doi: 10.1021/acscatal.9b01718
9. Kuribara T, Kaneki A, Matsuda Y, Nemoto T (2024) Visible-Light-Antenna Ligand-Enabled Samarium-Catalyzed Reductive Transformations. Journal of the American Chemical Society 146:20904-20912. https://doi.org/10.1021/jacs.4c05414
10. Ogura K, Nagai D, Okamoto S (2026) *N*,*N*-Dialkyl-1-pyrenylamine-Based Photoredox Catalysts for Light Driven Reductive Coupling of Aromatic Carbonyl Compounds and Imines. Journal of the Organic Chemistry 91:5428-5433. https://doi.org/10.1021/jacs.4c05414
11. Okamoto S, Nagai D (2024) Pyrene-Based Organic Photoredox Catalysts for Carbon−Carbon Bond-Forming Reactions: Reductive Coupling of Aromatic Carbonyl and Imine Compound*s*. Organic Letters 26:7718-7722. https://doi.org/10.1021/acs.orglett.4c02845
12. Das S, Kundu S, Metya A, Maji M S (2024) A Toolbox Approach to Revealing a Series of Naphthocarbazoles to Showcase Photocatalytic Reductive Syntheses. Chemical Science, 15:13466-13474. http:// doi: 10.1039/d4sc03438d
13. Huh H H, Lee Y J, Anita Y, Woo S K (2024) Visible-Light-Photocatalyzed Pinacol Coupling in Water. Asian Journal of Organic Chemistry, 13:e202300591. http:// doi.org/10.1002/ajoc.202300591
14. Calogero F, Magagnano G, Potenti S, Pasca F, Fermi A, Gualandi A, Ceroni P, Bergamini G, Cozzi P G (2022) Diastereoselective and Enantioselective Photoredox Pinacol Coupling Promoted by Titanium Complexes with a Red-Absorbing Organic Dye. Chemical Science, 13:5973-5981. http:// doi: 10.1039/d2sc00800a
15. Kundu S, Roy L, Maji M S (2022) Development of Carbazole-Cored Organo-Photocatalyst for Visible Light-Driven Reductive Pinacol/Imino-Pinacol Coupling. Organic Letters, 24:9001-9006.
16. Wang H, Qu J-P, Kang Y-B (2021) CBZ6 as a Recyclable Organic Photoreductant for Pinacol Coupling. Organic Letters, 23:2900-2903.
17. Yedase G S, John M, Yatham V R (2021) Organophotoredox-Catalyzed Switchable Selective Transformation of Aromatic Aldehydes into Pinacols and Benzyl alcohols. Asian Journal of Organic Chemistry, 10:2916-2920. http://

doi.org/10.1002/ajoc.202100516

18. Noto N, Hyodo Y, Yoshizawa M, Koike T, Akita M (2020) Transition Metal-Free Supramolecular Photoredox Catalysis in Water: A Phenoxazine Photocatalyst Encapsulated in V-Shaped Aromatic Amphiphiles. ACS Catalysis, 10:14283-14289. https://dx.doi.org/10.1021/acscatal.0c04221
19. Gualandi A, Rodeghiero G, Rocca E D, Bertoni F, Marchini M, Perciaccante R, Jansen T P, Ceroni P, Cozzi P G (2018) Application of coumarin dyes for organic photoredox catalysis. Chemical Communications, 54:10044-10047. https://doi: 10.1039/c8cc04048f
20. Zhang M, Rouch W D, McCulla R D (2012) Conjugated Polymers as Photoredox Catalysts: Visible-Light-Driven Reduction of Aryl Aldehydes by Poly(*p*-phenylene). European Journal of Organic Chemistry, 31:6187-6196. http://dx.doi.org/10.1002/ejoc.201200437.
21. Ito H, Sudo A (2021) Visible-light-driven reductive coupling of aromatic ketones using perylene derivatives as photoredox catalysts: Improvement of reaction efficiency by the addition of acetic acid. Results in Chemistry, 3:100123. https://doi.org/10.1016/j.rechem.2021.100123
22. Okamoto S, Tsujioka H, Sudo A (2018) Organic Photoredox Catalyst with Substrate-capture Ability: A Perylene Derivative Bearing Urethane Moiety for Reductive Coupling of Ketones and Aldehydes under Visible Light. Chemistry Letters, 47:369-372. https://doi.org/10.1246/cl.171160
23. Okamoto S, Kojiyama K, Tsujioka H, Sudo A (2016) Organic Photoredox Catalyst with Substrate-capture Ability: A Perylene Derivative Bearing Urethane Moiety for Reductive Coupling of Ketones and Aldehydes under Visible Light. Chemistry Letters, 47:369-372. https://doi: 10.1039/c6cc05867a
24. Wege V U, Greiner A (1995) New synthetic of OH-functionalized poly(*p*-xylylene)s by coupling of aromatic dialdehydes and diketones in the presence of Sm_2. Acta Polymerica, 46:391-395. https://doi.org/10.1002/actp.1995.010460507
25. Wang P-Z, Chen J-R, Xiao W-J (2019) Hantzsch esters: an emerging versatile class of reagents in photoredox catalyzed organic synthesis. Organic & Biomolecular Chemistry, 17:6936-6951. https://doi:10.1039/c9ob01289c
26. Merz J, Steffen A, Nitsch J, Fink J, Schürger C B, Friedrich A, Krummenacher I, Braunschweig H, Moos M, Mims D, Lambert C, Marder T B (2019) Synthesis, photophysical and electronic properties of tetra-donor- or acceptor-substituted orthoperylenesdisplaying four reversible oxidations or reductions. Chemical Science, 10:7516-7534. http:// doi: 10.1039/c9sc02420d

27. Noto N, Koike T, Akita M (2017) Metal-Free Di- and Tri-fluoromethylation of Alkenes Realized by Visible-light-induced Perylene Photoredox Catalysis. Chemical Science, 8:6375-6379. http:// doi: 10.1039/c7sc01703k
28. Luo J, Zhang X, Zhang J (2015) Carbazolic Porous Organic Framework as an Efficient, Metal-Free Visible-Light Photocatalyst for Organic Synthesis. ACS Catalysis, 5:2250-2254. http://doi: 10.1021/acscatal.5b00025
29. Roth H G, Romero N A, Nicewicz D A (2016) Experimental and Calculated Electrochemical Potentials of Common Organic Molecules for Applications to Single-Electron Redox Chemistry. Synlett, 27:714-723. http://doi: 10.1055/s-0035-1561297; Art ID: st-2015-r0838-c

Authors and Affiliations

Shusuke Okamoto[1]・Seito Nose[2]・Atsushi Sudo[2]

Atsushi Sudo
asudo@emat.kindai.ac.jp

[1] School of Food and Nutritional Science, University of Shizuoka, 52-1 Yada, Suruga-ku, Shizuoka, Shizuoka, 422-8526, Japan.
[2] Graduate School of Science and Engineering, Kindai University, Kowakae 3-4-1, Higashi Osaka, Osaka 577-8502, Japan.

Supplementary Files

This is a list of supplementary files associated with this preprint. Click to download.

- Supplementaryinformation.pdf